DETERMINATION OF CONDITIONS OF CAVITATION INCEPTION ON BODIES IN A FLOW WITH SEPARATION AND ATTACHMENT OF THE BOUNDARY LAYER

É. L. Amromin, V. K. Aleksandrov, and Yu. L. Levkovskii

UDC 532.533.528

The theory of an ideal fluid stream for the most part adequately describes large cavities behind such objects as disks, cones, wedges, etc. In engineering practice, however, the undesirable effects of cavitation makes it important to study its initial stages and, in particular, to determine the conditions for the inception of cavitation on a body or the cavitation number σ_i (i.e., the greatest value of the cavitation number σ corresponding to a very small cavity). The minimum pressure determines σ_i in an ideal fluid (for bodies with sharp edges, values $\sigma \to \infty$ are permitted [1, 2]). Tests (see [3-6], for example) show that apart from the dimensionless pressure coefficient C_p, the value of σ_i is heavily affected by the rate of flow about the body V and the size of the body D (or the Reynolds number Re and Weber number We constructed from V and D). The predictions of the theory of an ideal fluid stream differ from measurements especially for bodies characterized by flow with a separated boundary layer in a viscous fluid even in the absence of cavitation. However, no methods have been developed for calculating the scale effects associated with the inception of cavitation for such bodies. Here we propose a theory which makes it possible to determine the relations $\sigma_i(\mathrm{Re}, \mathrm{We})$ in those cases when the separated boundary layer becomes reattached to the body (i.e., for flow with separation bubbles). Results are presented from calculations of plane and axisymmetric flows for hydrofoils and nonlifting bodies and are compared with experimental data.

It is proposed that the calculation of $\sigma_i(\mathrm{Re}, \mathrm{We})$ be broken down into the operations of calculation of separated flow of a viscous fluid about a body with a given Re and determination of the conditions of equilibrium of a cavity in the separation zone with a given We. We modified the method described in [7] to calculate viscous separation, while the value of C_p and the width of the separation zone h which were calculated were used in determining σ_i from the Laplace formula

$$\sigma + C_p + 2r^{-1}\mathrm{We}^{-1} = 0. \qquad (1)$$

In the given flow scheme (Fig. 1) the radius of curvature of the boundary of the cavity $r = h/2$ at $\sigma = \sigma_i$ (at larger r the cavity begins to act as a barrier, so that there is an increase in the length of the separation zone and a decrease in $|C_p|$).

Features of the method of calculation of the flow are connected with the size of the tolerable error in the determination of the quantities in (1). The usual scatter of measurements of σ_i with fixed Re and We is at least 0.02-0.03, while a 20-40% change in We does not take σ_i outside this band. Since (1) contains the product rWe, we can calculate h and the characteristic thicknesses of the boundary layer with roughly the same error as We, but we can calculate C_p with considerably greater relative accuracy. Thus, in calculating the parameters of the flow in the separation region (i.e., in the region of strong viscous-inviscid interaction), the distribution of C_p is approximated more carefully here than in [7] and the separated boundary layer is described in less detail.

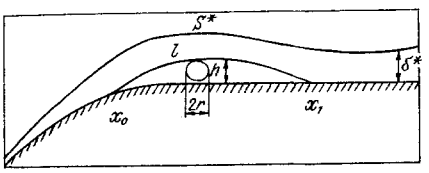

Fig. 1

Leningrad. Translated from Zhurnal Prikladnoi Mekhaniki i Tekhnicheskoi Fiziki, No. 2, pp. 34-40, March-April, 1986. Original article submitted December 14, 1984.

0021-8944/86/2702-0184$12.50

The usual assumptions for flows with viscous-inviscid interaction are made here in calculating flows with viscous separation: subdivision of the flow about the body into viscous and potential flows with the use of the notion of a displacement body [7, 8]; the absence of a pressure gradient across the viscous layer. The viscous flow affects the potential flow through the shape of their common boundary, while the potential flow influences the viscous flow through the distribution of C_p on it. In turn, as in [7], the viscous flow is subdivided into the boundary layer, the wake, and the stagnation zone. The latter is separated from the boundary layer by the line of zero friction ℓ. The boundaries between these flow regions and the quantities in the joining conditions written on the boundaries are not known beforehand. Thus, strictly speaking, the calculation should be performed by successive approximations.

The studies [2, 8, 9] described the methods of hydrodynamic features used in the present calculations of potential flow, as well as the integral methods used to calculate the boundary layer. Here we will examine only the modification of the method in [7] used to directly calculate flow in the separation zone. As regards calculations of potential flow and the boundary layer, it suffices for now to remember that they are used to determine the coupled Bernoulli integral $U^2_b - 1 = C_{pb}$ with the coefficient C_{pb}, the velocity of the potential flow U_b (on the boundary of the displacement body S determined in the previous approximation), and the displacement thickness δ^* near the point x_0, determined from local separation conditions [7, 8] and representing the beginning of the separation zone (in axisymmetric flow, S is the meridional section of the displacement body). We find x_0 from the Kochin–Loitsyanskii criterion (for a laminar layer) or the Bam–Zelikovich criterion (for a turbulent layer). It is also assumed that x_0 is the origin of the line of zero friction, while the functions $U_b(s)$ and $\delta^*(s)$ are continuous at $s = x_0$ together with their first derivatives. In contrast to [7], we do not introduce a zone of alternating separation. Meanwhile, the two-parameter method used to calculate the turbulent boundary layer makes it possible to perform calculations up to values of the form factor $H = \delta^*/\delta^{**} = 35/9$.

It is known from tests that the diagram of C_p along a separation bubble consists of two diffuser sections and a nearly isobaric zone between them. However, the total length of the separation zone L, the length of the sections just mentioned, and the distribution $U = (1 - C_p)^{0.5}$ are all unknown beforehand. If L and ℓ_1 and $L - \ell_2$ (the lengths of these sections in Fig. 2) were known, it would be possible (as in [10]), after representing U in the form of a linear combination of undetermined coefficients C_1, C_2, ... and some unknown functions, to first determine these coefficients from the conditions of separation and attachment of the boundary layer, then correct the boundary of the displacement body S from the difference $U - U_b$, and finally find h after integrating the equation of the separated boundary layer.

We write the local separation conditions at $s = x_0$ in the form

$$\frac{U'\delta^{*k+1}}{UD^k} + \frac{\alpha_k}{\mathrm{Re}^k} = 0, \tag{2}$$

while the conditions of attachment at $s = x_1$ (where ℓ is again attached to the body) are

$$U'\,\delta^* + 0.015\,U = 0; \tag{3}$$

$$R' = 0, \tag{4}$$

where $k = 1$ for the laminar layer and $k = 0$ for the turbulent layer; $\alpha_1 = 1.1$, $\alpha_0 = 0.015$; R is the distance between the boundary of the displacement body S* known from the previous approximation (the sample surface, to use the terminology in [2]) and the sought surface S on which the velocity should be equal to U; R is reckoned along an external normal to S*; the prime denotes differentiation along S*.

Condition (3), similar to that used in [11] and formally coinciding with the Bam–Zelikovich criterion, can be derived from the Prandtl equation in Clauser's form at the critical point on the zero-friction line with a value of 0.03 for the constant in this formula and, as in [7], with the use of the wake longitudinal-velocity profile

$$u(n) = u_0 + (U - u_0)(3\eta^2 - 2\eta^3) \tag{5}$$

in the separated boundary layer. Here u_0 is the velocity on ℓ, while η is its transverse coordinate referred to the thickness of the separated layer. Condition (4) ensures continuity of $\delta^{*\prime}$ at $s = x_1$ (and thus the possibility of solving the entire problem by successive approximations).

The single form of condition (3) for k = 0 and 1 is connected with the fact that a laminar-turbulent transition occurs in separation bubbles in the last case.

In the presence of only the three conditions (2)-(4), it is possible to find only three undetermined coefficients. As in [1, 2, 7], the relationship between R and the presumably small dimensions $U_b - U(s, C_1, C_2, C_3)$ can be expressed through the potential of a simple layer φ and simple formulas for linear inverse problems:

$$\Delta\varphi = 0; \tag{6}$$

$$\varphi' = U_b - U; \tag{7}$$

$$(RU_b)' + \partial\varphi/\partial N = 0. \tag{8}$$

Excluding q – the density of the potential φ – from (7) by means of (8), we can also represent R as a linear combination with the coefficients C_1, C_2, and C_3. Here, (4) reduces to the condition of boundedness of the function $q_1(s) = q(s) - q_0(s)$:

$$\int_{x_0}^{x_1} \frac{\varphi'(q_0, s) + \varphi'(q_1, s) + 0{,}5\, I_k(q_1, s) + U(s) - U_b(s)}{[(x_i - s)(s - x_0)]^{0,5}}\, ds = 0. \tag{4a}$$

Here, I_k is the Cauchy density integral q_1, determined at $x_0 < s < x_1$, while the familiar function $q_0(s)$ is chosen so as to satisfy (8) at $s = x_0$. The quantity R is equal to the difference between the values of δ^* in two successive approximations (in the first approximation it is simply the value $\delta^*(x_0)$, while in the linear approximation $q_0(x_0) = 2[\delta^* U_b]'|_{s=x_0}$). Picking out I_k makes it possible to later use the Keldysh–Sevod formula for regularization of (7).

At $s = x_1$, in accordance with the concept of a displacement body, the following condition should also be satisfied:

$$R = \delta^* - \delta_0^*, \tag{9}$$

where δ^*_0 is the value of δ^* calculated in the previous approximation at $s = x_1$ (in the first approximation, $\delta^*_0 \equiv 0$). Thus, in the calculations it turns out to be convenient to express δ^* in (3) through R by means of (9) and to in turn express $R(x_1)$ through C_1, C_2, and C_3 with the use of (6)-(8). We then solve system (2)-(4a), consisting of one quadratic and two linear equations in these undetermined coefficients.

After C_1, C_2, and C_3 are determined by means of (6)-(8), we can find S.

We find L by means of Eq. (9), the left side of which is calculated by the above-described method from the difference $U - U_b$ with the use of linearized equations of potential theory. The value of δ^* is calculated by means of the Karman equation on ℓ

$$U\delta^{**\prime} + U'\delta^{**}(2 + H) = 0. \tag{10}$$

Having taken the profile (5) for u above ℓ, we can write $H = 35/(9 + 26u_0/U)$. The function $u_0(s)$ is approximated on the basis of the measurements from [12].

We find the length ℓ_1 in accordance with the measurements in [6, 7] and the asymptotic representations from [13]:

$$\frac{l_1}{D} = \frac{85kx_0}{\mathrm{Re}^{0,625}} + 2\,\frac{(1-k)\,\delta^*(x_0)}{\mathrm{Re}^{0,03}} \tag{11}$$

(the arc abscissa x_0 is reckoned from the critical point). The length of the isobaric section $\ell_2 - \ell_1$ is determined from a variational principle similar to that formulated in [14] for cavitating flows: $J = U^2\delta^{**}$ is minimized at $s = x_1$.

Thus the overall order of the calculations after the determination of U_b, x_0, ℓ_1, and δ^* and $\delta^{*\prime}$ at $s = x_0$ is as follows: Eq. (9) is regarded as an equation in L and is solved by Newton's method; with a fixed L, the length ℓ_2 is chosen so that J is minimized; with fixed ℓ_1, ℓ_2, and L, the values of C_1, C_2, C_3, and R(s) are calculated and Eq. (10) is integrated; the error in (9) is calculated, and so on. When the process converges, the function $C_p(\mathrm{Re}, s)$ will be determined. Then, to calculate $\sigma_i(\mathrm{Re}, \mathrm{We})$, as h in Eq. (1) we take the maximum distance between ℓ and the surface of the body within the isobaric section of the separation zone;

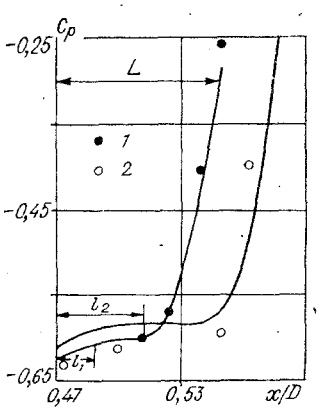

Fig. 2

then, having evaluated the convergence with respect to σ_i, we can either complete the calculation or, having calculated the layer at $s > x_1$ and the viscous wake, proceed to a new approximation.

However, we used only one approximation in the given calculations, and the viscous flow at $s > x_1$ was not calculated. Meanwhile, as U_b we took the velocity of potential flow about the body itself. The edges of the body are rounded before calculating U_b only for bodies with sharp edges in order to ensure the smallness (compared to V) of the right side of (7), as in calculations of cavitation in an ideal fluid [2]. For the profiles in finding C_{pb}, it is necessary to correct the relationship between the buoyance coefficient C_y and the angle of attack α by means of the corrections for the effect of viscosity described in [15]. The effect of constraint of the flow in pipes on U_b (to compare the calculations with the measurements in [5, 6]) is considered by the method described in [2].

In the present calculations, we took U(s) in the form

$$U(s) = \begin{cases} C_1(s - x_0 - l_1)^2 + C_2 & \text{at } x_0 \leqslant s < x_0 + l_1, \\ C_2 & \text{at } x_0 + l_1 \leqslant s \leqslant x_0 + l_2, \\ C_2 + C_3(s - x_0 - l_2)^2 & \text{at } x_0 + l_2 < s \leqslant x_1. \end{cases} \tag{12}$$

In connection with the importance of the calculation of C_p, it is best to compare calculated and measured diagrams of pressure along the separation zone. Figure 2 offers such a comparison for a body with a long cylindrical part and having the diameter D = 0.05 m and a hemispherical nose. The experimental points were taken from [6] and were enumerated in the same manner as the theoretical curves (1, V = 21 m/sec; 2, V = 9 m/sec). The abscissa x of the cylindrical coordinate system is reckoned from the critical point. The agreement between the theory and experiment in particular confirms the validity of Eq. (12) for U, as well as the adequacy of a single approximation to satisfactorily determine the dimensions of the separation bubble and the distribution of C_p along its boundary. Such good agreement is related to the relatively small thickness of the bubble in these examples. Thus, the pressure gradient across the layer makes a small contribution to the value of C_p in (1). However, the calculating procedure described leaves open the possibility of gradual refinement of the position and shape of the separation zone and the parameters of the boundary layer ahead of it; here it is possible to make use of the experience in [2, 10] in the solution of nonlinear problems for developed cavitation; also, using the relations presented in [16] and the method described here, it would also be possible to consider the effect of a transverse pressure gradient in the Karman equations and Laplace formula – such operations do not cause any basic problems.

Figure 3 compares theoretical values of $\sigma_i(\mathrm{Re})$ for solids of revolution with measured values. The three theoretical curves pertain to three bodies with long cylindrical parts and identical D = 0.05 m but different noses. Curves 1 and 2 correspond to nose cones with cone angles of 45 and 90°, while curve 3 corresponds to a DTNSRDC body, the meridional section of which is described by the following formula for $x \in [0, D/2]$:

$$y = D/6\{2 + [1 - 2(x/D - 1)^2]^{0,5}\},$$

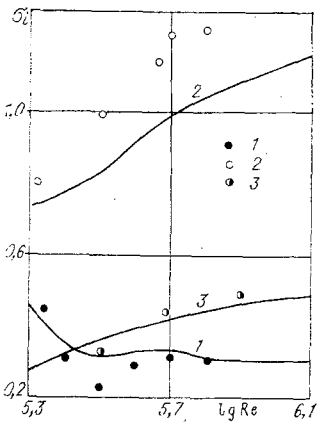

Fig. 3

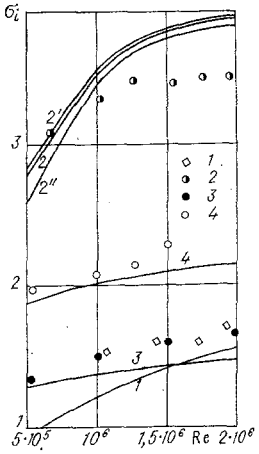

Fig. 4

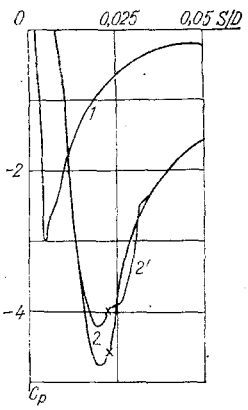

Fig. 5

while at x = 0 a segment of the length D/3 is parallel to the y axis. The experimental points corresponding to curves 1 and 2 were taken from [5], while those for curve 3 were taken from [6]. A substantial part of curve 1 and the experimental points on it correspond to the development of cavitation in the zone of turbulent separation, and $\sigma_i \to$ const with an increase in Re. The satisfactory agreement of curve 1 with the measurements in [5] indirectly confirms the closeness of the calculated and measured diagrams of C_p in the turbulent separation zone. Curves 2 and 3 correspond fully to laminary separation. At Re $\geq 10^6$-$1.5 \cdot 10^6$, a laminar-turbulent transition takes place on the nose of the DTNSRDC body and turbulent separation is not seen; for this body, $|\min C_p| \cong 0.88$.

Figure 4 shows σ_i(Re) for plane flows. Curves 3 and 4 represent the results of calculations for an NACA-16012 hydrofoil with $\alpha = 4$ and 6°. Experimental points 3 and 4 were taken from [4]; the value of σ_i constructed from the minimum of C_p (i.e., without allowance for the effect of viscosity and capillary) for 6°, for example, would have exceeded 3. Curves and experimental points 1 and 2 correspond to symmetrical KA-4 and KA-5 hydrofoils with $\alpha = 0$. Curves 1 and 2 in Fig. 5 for the diagrams of C_{pb} for these profiles show that they have the pressure distribution typical of sections of vanes of screw propellers (with the same local Reynolds numbers); D = 0.2 m for both hydrofoils. The increasing difference between the theory proposed here and the experimental results at Re > 10^6 for these hydrofoils may be connected not only with its approximate nature, but with the difficulty of observing very small cavities.

The calculations for the KA-4 and KA-5 hydrofoils were used to check approximations (11). Curve 2' corresponds to the length ℓ_1, reduced by half compared to that determined by (11), while curve 2" corresponds to double this value; the results show that even such a change in ℓ_1 is unimportant. As regards the use of a small amount of experimental data to approximate u_0, it must be noted that, as in [7], calculation of H from the ejection equation runs up against the problem of assigning the mixing coefficient along the separation bubble.

Curve 2' represents the C_p diagram at Re = 10^6 for the KA-5 hydrofoil. The x's on curves 2 and 2' denote values of C_{pb} and C_p at the beginning of the separation zone; these values already differ appreciably and, as follows from (1), σ_i differs from $|C_{pb}|$ even more. Thus, the recommendations in [6, 15] to take $|C_{pb}|$ for σ_i are not to be followed. We could not compare the estimates of σ_i obtained here with other estimates since no similar calculations have been performed.

Thus, qualitative agreement was obtained between calculated and measured values of σ_i for all of the bodies and hydrofoils examined, and there is good quantitative agreement for some of them. Consequently, there is hope for future refinement of the theory [by improving the method of finding H for (10) or by increasing the number of approximations, for example] within the framework of the model described here.

We thank A. V. Vasil'ev and A. N. Ivanov for their useful discussions and help in the work.

LITERATURE CITED

1. L. I. Sedov, Continuum Mechanics [in Russian], Nauka, Moscow (1976), Pt. II.
2. A. N. Ivanov, Hydrodynamics of Developed Cavitating Flows [in Russian], Sudostroenie, Moscow (1980).
3. H. Lindgren and C.-A. Johnson, "Cavitation inception on headforms ITTS comparative experiments," in: 11th International Towing Tank Conference Report of Cavitation Comm., Tokyo (1966).
4. J. H. J. van Meulen, "Boundary layer and cavitation studies of NACA-16012 and NACA-4412 hydrofoils," in: 13th Symposium on Naval Hydrodynamics, Tokyo (1980).
5. S. Pan, Z. Yang, and P. Hsu, "Calculation inception tests on axisymmetric headforms," Trans. ASME J. Fluids Eng., 103, No. 2 (1981).
6. W. Holl and A. J. Caroll, "Observation of the various types of limited cavitation on axisymmetric bodies," Trans. ASME J. Fluids Eng., 103, No. 3 (1981).
7. L. V. Gogish and G. Yu. Stepanov, Turbulent Separated Flows [in Russian], Nauka, Moscow (1979).
8. L. G. Loitsyanskii, Mechanics of Liquids and Gases [in Russian], Nauka, Moscow (1971).
9. V. V. Droblenkov and G. I. Kanevskii, "Effect of the introduction of small polymer additions into a flow on the hydrodynamic characteristics of planar vanes," Izv. Akad. Nauk SSSR, Mekh. Zhidk. Gaza, No. 6 (1981).
10. É. L. Amromin and A. N. Ivanov, "Determination of the separation point of a cavitation cavity with allowance for capillarity and viscosity of the fluid," Dokl. Akad. Nauk SSSR, 264, No. 4 (1982).
11. W. B. Roberts, "Calculation of laminar separation bubbles and their effect on airfoil performance," AIAA J., 18, No. 1 (1980).
12. R. L. Simpson, Y.-T. Chew, and B. G. Shivaprasad, "The structure of a separating turbulent boundary layer, 1," J. Fluid Mech., 113 (1981).
13. L. V. Gogish, V. Ya. Neiland, and G. Yu. Stepanov, "Theory of two-dimensional separated flows," Itogi Nauki Tekh. Gidromekhanika, 8 (1975).
14. D. Riabouchinsky, "Sur une probleme de variation," C. R. Acad. Sci., No. 185 (1927).
15. Screw Propellers. Modern Methods of Design [in Russian], Sudostroenie, Leningrad (1983).
16. L. V. Gogish and G. Yu. Stepanov, "Turbulent separated flows," Izv. Akad. Nauk SSSR, Mekh. Zhidk. Gaza, No. 2 (1982).